Formation of stress-specific p53 binding patterns is influenced by chromatin but not by modulation of p53 binding affinity to response elements[†]

Jean-François Millau[1], Omari J. Bandele[2], Josiann Perron[1], Nathalie Bastien[1], Éric F. Bouchard[1], Luc Gaudreau[3], Douglas A. Bell[2] and Régen Drouin[1],*

[1]Division of Genetics, Department of Pediatrics, Faculty of Medicine and Health Sciences, Université de Sherbrooke, Sherbrooke, QC J1H 5N4, Canada, [2]Environmental Genomics Group, Laboratory of Molecular Genetics, National Institute of Environmental Health Sciences, Research Triangle Park, North Carolina, USA and [3]Department of Biology, Faculty of Sciences, Université de Sherbrooke, Sherbrooke, QC J1K 2R1, Canada

ABSTRACT

The p53 protein is crucial for adapting programs of gene expression in response to stress. Recently, we revealed that this occurs partly through the formation of stress-specific p53 binding patterns. However, the mechanisms that generate these binding patterns remain largely unknown. It is not established whether the selective binding of p53 is achieved through modulation of its binding affinity to certain response elements (REs) or via a chromatin-dependent mechanism. To shed light on this issue, we used a microsphere assay for protein–DNA binding to measure p53 binding patterns on naked DNA. In parallel, we measured p53 binding patterns within chromatin using chromatin immunoprecipitation and DNase I coupled to ligation-mediated polymerase chain reaction footprinting. Through this experimental approach, we revealed that UVB and Nutlin-3 doses, which lead to different cellular outcomes, induce similar p53 binding patterns on naked DNA. Conversely, the same treatments lead to stress-specific p53 binding patterns on chromatin. We show further that altering chromatin remodeling using an histone acetyltransferase inhibitor reduces p53 binding to REs. Altogether, our results reveal that the formation of p53 binding patterns is not due to the modulation of sequence-specific p53 binding affinity. Rather, we propose that chromatin and chromatin remodeling are required in this process.

INTRODUCTION

p53 controls cell fate in response to stress and is one of the first barriers against the process of carcinogenesis. In response to stress, p53 binds to its response elements (REs), which follow the pattern 5′-RRR CWWGYYYnRRRCWWGYYY-3′ (R = purine; Y = pyrimidine; W = adenine or thymine), and then regulates the transcription of genes involved in major cellular pathways (1–3). Depending on the stress context, p53 induces reversible cell cycle arrest, senescence, or apoptosis (4).

How p53 triggers stress-specific responses is an unresolved question (5). One hypothesis proposes that in response to a given stress, p53 binds only to the REs located near or within genes that need to be regulated, leading to stress-specific p53 binding patterns (see reference 6 for a review on mechanisms of transcription factor selectivity). Until now, this model remained challenged by the observation that, independent of the type of stress, p53 binds to most of its REs in cell lines (7,8). However, a recent report revealed that the absence of stress-specific p53 binding patterns might be a feature of cell lines (9,10). Moreover, using *p21* and its five p53 REs as a model gene, we showed that stress-specific p53 binding patterns actually occur in human primary cells and correlate with specific p21-variant transcription profiles (11). The fact that 15% of validated p53 effector genes contain multiple p53 REs suggests that this type of regulation might occur at multiple other genomic loci (3). Altogether, these observations emphasize the fact that p53 binding patterns are an important mechanism for the regulation of p53 effector genes and the adaptive response to stress.

Currently, little is known about the formation of these stress-specific p53 binding patterns. Evidence suggests that posttranslational modifications and/or targeting co-factors favor p53 binding to specific REs. For example, UV-induced Ser46 phosphorylation directs p53 to the promoter of pro-apoptotic genes (12), and Lys320 acetylation favors p53 binding to cell-cycle-arrest gene promoters (13). Moreover, targeting co-factors ASPP1, ASPP2 and BRN3B favor p53 binding to pro-apoptotic genes while iASPP, Hzf and BRN3A have the opposite effect (14–19). However, how these selective bindings are achieved remains largely unknown. Importantly, it is not known whether stress-induced p53 binding patterns are caused by the modulation of p53′s binding affinity to RE sequences or through a chromatin-dependent mechanism.

To shed light on this issue, we exposed human normal primary and human Li-Fraumeni fibroblasts to different doses of UVB or Nutlin-3 in order to generate different p53 binding patterns and distinct cellular outcomes. We then measured p53 binding activity on naked DNA with a microsphere assay for protein–DNA binding (MAPD) (20). This multiplexed test uses nuclear extracts to quantify p53 binding to oligonucleotides containing REs. Thus, while the nuclear protein context is preserved, MAPD overcomes the effect of chromatin to assessing whether p53 binding affinity to specific RE sequences is modulated in a stress-dependent manner. In parallel, we also measured p53 binding patterns in cells on chromatinized DNA. We used chromatin immuno-precipitation (ChIP), which reveals the presence of a protein within a given region of genomic DNA, as well as DNase I digestion coupled to ligation-mediated polymerase chain reaction (PCR) footprinting (DLF), which maps protein–DNA interactions at single-nucleotide resolution and establishes the occupancy status of a RE. The combination of these techniques allowed us to investigate the influence of chromatin on the formation of p53 binding patterns. Finally, remodeling of chromatin by acetylation of nucleosomal histones is an important mechanism that regulates gene expression (21). Using the histone acetyltransferase inhibitor (HATi) Garcinol, which inhibits the histone acetyltransferases (HAT) p300 and pCAF, we investigated whether chromatin remodeling is involved in the regulation of p53 binding to REs (22).

In this article, we show that stress-specific p53 binding patterns are not caused by modulation of p53 binding affinity to specific REs. Rather, chromatin and chromatin remodeling appear to make significant contributions to the regulation of p53 binding activity and the formation of p53 binding patterns.

MATERIALS AND METHODS

Cells and cell culture

Human normal primary skin fibroblasts (considered wild-type fibroblasts or wt) and human Li-Fraumeni (LF) skin fibroblasts (LF041 strain, a gift from M. Tainsky, University of Texas M. D. Anderson Cancer Center, Houston, TX, USA) were grown in Dulbecco's Modified Eagle Medium (DMEM) containing 10% FBS, 0.2 U/mL penicillin G and 100 μg/mL streptomycin, all from Wisent Bioproducts (St. Bruno, QC, Canada). LF041 fibroblasts have lost one *p53* allele and carry a frameshift mutation at codon 184 in the remaining copy.

Cell treatments

UVB irradiations of 250, 500 and 2000 J/m^2 were performed with FS20T12/UVB/BP tubes (Philips, Franklin Square Drive, NJ, USA); wavelengths below 290 nm were filtered by a clear 0.015-inch Kodacel TA-407 (Eastman Kodak, Rochester, NY, USA). The dose was measured using a UVX Digital Radiometer (UVP Inc., Upland, CA, USA). Induction of p53 in the absence of stress was carried out using 1, 2.5 and 10 μM of Nutlin-3 (Sigma, St. Louis, MO, USA). For the inhibition of histone acetyltransferase (HAT), cells were treated with 10, 25 and 50 μM of Garcinol (Sigma, St. Louis, MO, USA) for 2 h, then irradiated with UVB and reincubated for 12 h in the presence of Garcinol.

Cell-cycle analysis

DNA was stained using DAPI as previously described (23). DAPI fluorescent signal was quantified by laser scanning cytometry (LSC) using the iCys Research Imaging Cytometer (Compucyte, Cambridge, MA, USA) (11). A minimum of 1500 cells per experimental condition were analyzed and experiments were performed in triplicate.

Cell proliferation

5×10^4 cells were seeded 24 h prior to UVB or Nutlin-3 treatments. For UVB, cells were counted 2 and 6 days after irradiation. For Nutlin-3, cells were treated for 24 h and then grown in Nutlin-3 free medium until counting on Days 2 and 6. Experiments were performed in triplicate.

Measurement of apoptotic cells

Fibroblasts were plated 24 h prior to UVB irradiation or incubation with Nutlin-3 for 24 h. Cells were then harvested 48 h post-treatment and cells were stained using the Vybrant 3 apoptosis kit (Molecular Probes, Eugene, OR, USA). Apoptotic cells were then quantified using a FACScan (Becton Dickinson, San Jose, CA, USA).

p21 mRNA quantification

The measurement of p21 mRNA was performed by qPCR as previously described (11).

Microsphere assay for protein–DNA binding

Oligonucleotides for MAPD (Invitrogen, Carlsbad, CA, USA) consisted of a forward oligonucleotide composed of 5′ 'anti-tag' sequences followed by p53 REs flanked with 45 nt of their respective genomic sequences (Table S1). The forward oligonucleotide was hybridized to a unique 'tag' sequence on each MicroPlexTM-xTAG microsphere (Luminex, Austin, TX, USA). The reverse oligonucleotide was complementary to the forward

strand and biotinylated on 5′. Forward and reverse oligo-nucleotides and MicroPlexTM-xTAG microspheres were hybridized as previously described (20).

To evaluate p53 binding patterns, nuclear extracts were prepared using the nuclear-extract kit from Active Motif (Carlsbad, CA, USA) and p53 binding was measured using the MAPD assay as previously described (20,24). A non-binding sequence (negative control WRNC) and a positive binding sequence [positive control ConC GGGCAA GTCTGGGCAAGTCT, which is a perfect match with the p53 consensus RE (25,26)] were examined in each reaction, untreated cells served as a negative control. Microspheres were multiplexed and added to p53 binding buffer supplemented with a non-competing double-stranded oligonucleotide (TransAm p53 kit, Active Motif, Carlsbad, CA, USA). Beads were incubated for 1 h in the presence of 5 µg of nuclear extracts. Microspheres were then incubated for 30 min with primary antibodies against p53 followed by a 30-min incubation with phycoerythrin-conjugated secondary antibodies. Fluorescence intensity was measured by flow cytometric analysis using a Bio-Plex® 200 System (Bio-Rad, Hercules, CA, USA). p53 binding fluorescence was normalized as previously described (20).

Immunoblotting

The blots were probed with primary antibodies (Santa Cruz Biotechnology, Inc., Santa Cruz, CA, USA) for p53 (DO-1) and actin (C-11). Bands were detected using horseradish peroxide-conjugated secondary antibodies (Santa Cruz) and the ECL Western Blotting System (Amersham Biosciences, Piscataway, NJ, USA).

Chromatin immunoprecipitation

ChIP assays were performed as previously described (27). Samples were sonicated to generate 500-bp DNA fragments. Immunoprecipitations were carried out using anti-p53 antibody DO-1 from Santa Cruz Biotechnology (Santa Cruz, CA, USA), anti-H3 antibody from Abcam (Cambridge, MA, USA), and anti-acetyl-H3 and anti-acetyl-H4 antibodies from Millipore (Billerica, MA, USA). Preimmune and no antibody controls were also performed. qPCR was done using the primer sets specific for the p53 REs located on *p21* (Table S2). ChIP experiments were performed in duplicate.

DNase I coupled to ligation-mediated PCR footprinting

DNase I footprinting reaction was carried out as previously published (11,28). The p53 REs located on *p21* were studied using the primer sets reported in Table S3. We used ImageQuant 5.0 (Molecular Dynamics, Sunnyvale, CA, USA) to quantify sequencer TIF files (Figure S1) and determine gel-band-intensity profiles. Data were first corrected for the gel background fluorescence. For each lane, we then calculated the average band-intensity outside of the footprint area (ABIout). The ABIout was then used to normalize intensity between non-treated and treated lanes. The ratio between ABIout of non-treated lanes and treated lanes to be corrected was computed and used to normalize the intensity of treated lanes to that of the non-treated lane. Bands were identified by the presence of a local intensity maximum. Band-intensity was calculated by adding the intensity values of the 5 pixels centered on the local intensity maximum of the band. Band-intensity ratios between treated and non-treated samples were then computed, also as the 5-band-interval mobile averages (Figure S2). Negative-footprint-intensity averages were calculated by averaging the mobile-average values encompassed in the RE sequence.

RESULTS

Choice of treatments and doses

In order to induce unique p53 binding patterns, we exposed human primary fibroblasts to distinct treatments and treatment doses. We used 250, 500 and 2000 J/m^2 UVB to induce p53 accumulation following genotoxic stress. As a control, we used 1, 2.5 and 10 µM Nutlin-3 to induce p53 accumulation in the absence of stress context through the inhibition of p53-MDM2 interactions. Interestingly, UVB leads to a plethora of well-characterized p53 posttranslational modifications (29), while Nutlin-3 induces few modifications of p53 (30,31). Thus if p53 affinity to REs is modulated in a stress-specific context (e.g. posttranslational modifications or co-factors) and stress intensity, one would expect that these treatment conditions will generate distinct p53 binding patterns.

UVB and Nutlin-3 treatments lead to different cellular outcomes

We first verified the effect of treatment doses on cellular outcomes. Wild-type (wt) and LF fibroblasts were treated with UVB and Nutlin-3 doses and cell cycle, cell proliferation and apoptosis were monitored (Figure 1).

UVB doses induced different cell-cycle-arrest responses. In wt fibroblasts, a G1/S arrest was observed following 250 J/m^2 while 500 J/m^2 arrested cells in G2/M and 2000 J/m^2 did not affect the cell cycle (Figure 1A). In LF fibroblasts, both 250 J/m^2 and 500 J/m^2 doses induced a G2/M arrest while 2000 J/m^2 had no effect on cell-cycle progression. The UVB doses also affected cell proliferation differently. In wt fibroblasts, cell growth was reduced following 250 J/m^2, arrested by 500 J/m^2, and apoptosis was induced at 2000 J/m^2 (Figure 1B and C). The absence of p53 in LF fibroblasts sensitized the cells to UVB. The 250 J/m^2 dose strongly reduced cell growth while 500 and 2000 J/m^2 induced apoptosis (Figure 1B and C).

The cell response to Nutlin-3 led to a decrease in S phase cells through a G1/S arrest in wt fibroblasts only (Figure 1A). Cell proliferation was reduced as Nutlin-3 concentration increased but the highest dose was not sufficient to stop cell growth entirely and no apoptosis was observed (Figure 1B and C).

Thus, 250, 500 and 2000 J/m^2 UVB induced transient cell-cycle arrest, permanent cell-cycle arrest and apoptosis, respectively, while 1, 2.5 and 10 µM Nutlin-3 only induced cell-cycle arrests.
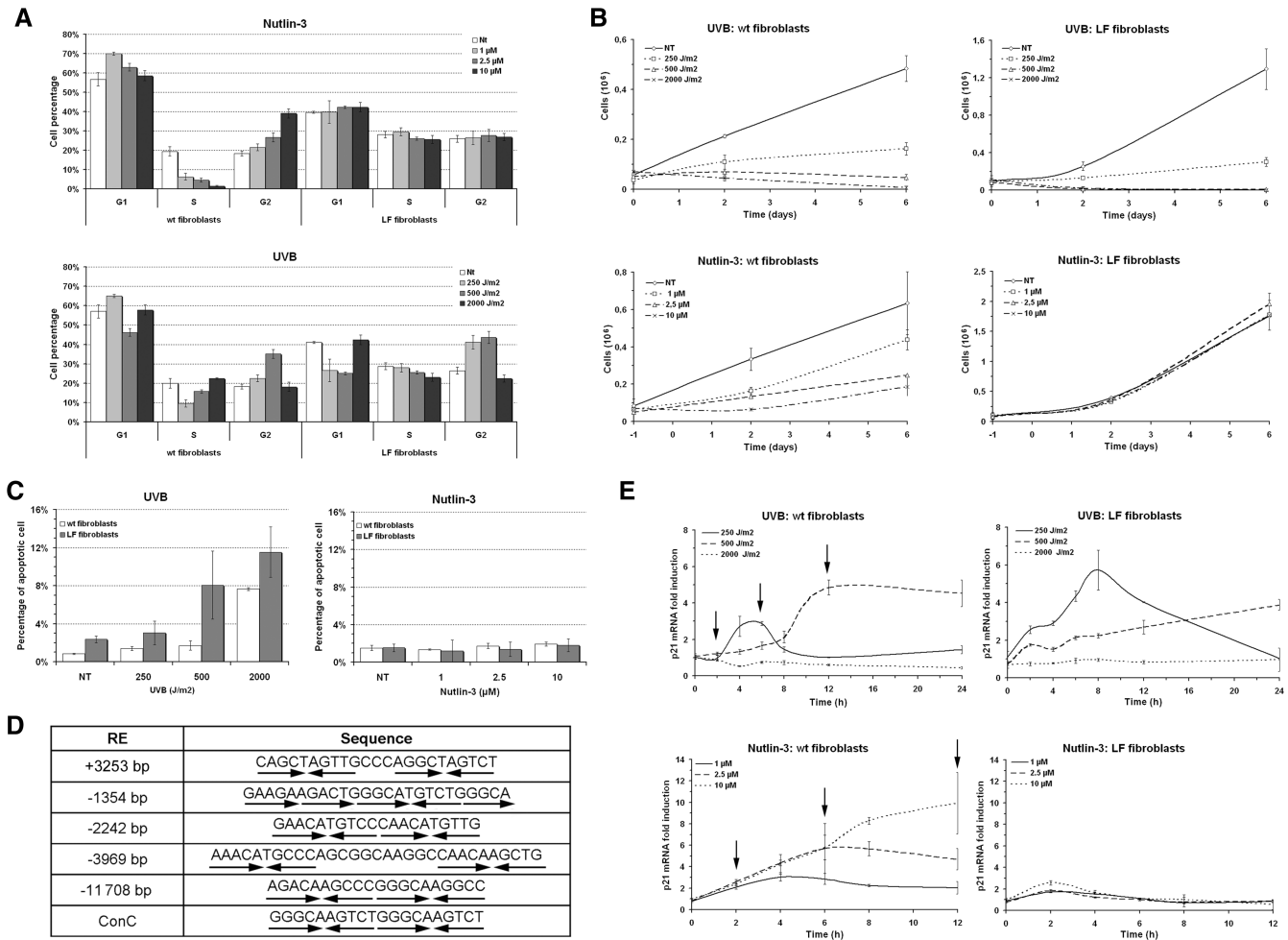
Figure 1. UVB and Nutlin-3 treatment doses induce different cellular outcomes and transcription of *p21*. (**A**) Measurement of cell cycle. wt and LF fibroblasts were exposed to UVB and Nutlin-3 and the percentage of cells in each phase was determined 24-h post-treatment. (**B**) Measurement of cell proliferation. wt and LF fibroblasts were exposed to UVB and Nutlin-3 and cells were counted at Day 2 and Day 6. (**C**) Measurement of apoptotic cells. wt and LF fibroblasts were exposed to UVB and Nutlin-3 and apoptotic cells were measured 48 h post-treatment. (**D**) Sequences of the different p53 RE located on the *p21* gene, arrows indicate RE pentamers orientations. (**E**) Measurement of p21 mRNA induction kinetic. wt fibroblasts and LF fibroblasts were exposed to UVB and Nutlin-3 and mRNA were analyzed by means of qPCR. Arrows indicate the induction times retained to measure p53 transcriptional binding activities. Note: All experiments were performed in triplicate and data are presented as mean ± SD.

Different *p21* transcription profiles are induced by UVB and Nutlin-3 treatments

In order to study p53 binding patterns on different REs, we used *p21* and the five p53 REs located at +3253, −1354, −2242, −3969 and −11 708 bp from its transcription start site as a model gene (Figure 1D) (7,32–34). We followed p21 mRNA levels to determine the best time conditions to measure p53 transcriptional binding activities and to investigate whether the different cellular outcomes were correlated with specific *p21* transcription profiles.

UVB treatment doses induced three distinct p21 mRNA transcription profiles that correlated with the three different cellular outcomes (Figure 1E). p21 mRNA induction was lower and shorter in wt fibroblasts than in LF fibroblasts following $250 \, \text{J/m}^2$, indicating that the presence of p53 repressed *p21* transcription. The $500 \, \text{J/m}^2$ dose led to p53-dependent induction of p21 mRNA only after 8 h in wt fibroblasts when compared with LF fibroblasts. No

augmentation of p21 mRNA level was observed following $2000 \, \text{J/m}^2$ in wt or LF fibroblasts. Finally, Nutlin-3 exposure increased p21 mRNA levels in a dose-dependent manner only in wt fibroblasts (Figure 1E). Based on these transcription profiles, we decided to study p53 transcriptional activities at 2, 6 and 12 h.

UVB and Nutlin-3 treatment doses lead to similar p53 binding patterns on naked DNA

We wondered whether the formation of p53 binding patterns is caused by a stress-dependent regulation of p53 binding affinity to specific RE sequences. To answer this question, we measured p53 binding activity to the five REs of *p21* in a naked DNA context using the MAPD assay and nuclear extracts of fibroblasts treated with Nutlin-3 or UVB doses (20). We observed the most intense binding with $500 \, \text{J/m}^2$ UVB and $10 \, \mu\text{M}$ Nutlin-3 (Figures 2A and S3). For each Nutlin-3 dose, p53 binding increased in a time-dependent manner and was maximal at

12 h, while UVB-induced p53 binding reached a maximum at 6 h and decreased at 12 h for all REs (Figures 2A and S3). Since p53 protein level remained high at 12 h following UVB (Figure S4), which suggests that p53 binding activity was globally inhibited at this time, after 6 h, UVB and Nutlin-3 induced similar binding intensities between REs. The −1354 and −2242 bp REs were highly bound by p53 similar to the positive control ConC, while the −3969 and −11 708 bp REs displayed less pronounced levels of p53 binding (Figure 2A). Strikingly, no p53 binding to the +3253 bp RE was observed. Using DLF, we previously reported that we were not able to measure p53 binding to this RE in cells (11). Thus, this sequence may not be a *bona fide* p53 RE or is a very low affinity RE.

Subsequently, we investigated the effect of treatment doses on p53 binding patterns. We used scatter plot representation of data to compare the binding patterns obtained following UVB and Nutlin-3 doses. If binding patterns are similar, the RE binding intensities from two different conditions result in a correlation factor (R^2) close to 1. As seen in Figure 2B, the p53 binding patterns obtained were similar for the different UVB doses tested despite the different cellular outcomes they generated (R^2 values ranged from 0.89 to 0.98). Only the global binding activity to all REs varied among UVB conditions, which is reflected by regression-line slopes (m) different from 1 and from each other (Figure 2B). Similar observations were made following Nutlin-3 treatments. p53 binding patterns were comparable between the different Nutlin-3 doses since R^2 values ranged from 0.83 to 0.99 (Figure 2B).

We then asked whether UVB- and Nutlin-3-induced p53 binding patterns were different. We compared the p53 binding obtained for the different UVB doses with the 10 μM Nutlin-3 dose (Figure 2C). The UVB doses yielded similar p53 binding patterns to 10 μM Nutlin-3 (R^2 values ranging from 0.77 to 0.95). The same observations were made when we compared the UVB doses with 1 or 2.5 μM Nutlin-3 (Figure S5).

Finally, we wondered whether these observations were valid for REs located near other genes. Using MAPD, we measured p53 binding activities on the −83 bp and +354 bp REs of *Bax* and the +762 bp and +724 bp REs of *MDM2* (Figure S6). We obtained R^2 values close to 1, indicating that these REs were also bound similarly following exposure to Nutlin-3 and UVB doses. Altogether, these data led to the conclusion that different treatment doses, which lead to different cellular outcomes, induce similar p53 binding patterns on naked DNA. This suggests that p53 binding affinity to specific RE sequences is not a function of the type of stress experienced by the cell.

UVB and Nutlin-3 treatments induce stress-specific p53 binding patterns in cells on chromatinized DNA

Since no p53 binding patterns were observed on naked DNA, we then investigated whether stress-specific p53 binding patterns are scored within chromatin. To this end, we used ChIP and DLF to measure p53 binding

patterns on the REs located in *p21* in fibroblasts following exposure to 500 J/m² UVB and 10 μM Nutlin-3 (Figure 3). We selected these treatment doses because they induced high and comparable p53 binding intensities on naked DNA (m = 0.94, Figure 2C).

Initially, measurement of p53 binding activity by ChIP revealed that Nutlin-3 and UVB treatments led to similar p53 binding patterns within chromatin (Figure 3). However, these data differed to what we observed on naked DNA by several key points. For example, p53 was located at the −1354, −2242 and −11 708 bp REs, but was never found associated to the −3969 bp RE although p53 bound this RE on naked DNA (Figures 2A and 3). Moreover, in contrast to the results obtained with the −2242 bp RE, p53 binding to the −1354 bp RE was less intense on chromatin than on naked DNA (Figures 2A and 3). Finally, while p53 binding activities were strongly reduced at 12 h following UVB, as measured by MAPD (Figure 2A), ChIP revealed substantial p53 binding to REs at this time in cells.

Since no stress-specific p53 binding patterns were observed using ChIP, we used DLF to precisely investigate the occupancy status of p53 REs (35). We did not observe any footprints in LF fibroblasts (data not shown) (11). In wt fibroblasts, footprints were identified for the −1354, −2242 and −11 708 bp REs but not the −3969 bp RE, which confirmed the ChIP results (Figure 3). However, following Nutlin-3 treatments, p53 was detected at the −11 708 bp RE by ChIP, but no occupancy of this RE was measured by DLF. Although DLF is less sensitive than ChIP (footprints are rarely observed below 0.1% of ChIP input), we ruled out any sensitivity issue regarding this result since DLF was capable of measuring p53 binding to the −11 708 bp RE following UVB. Thus, conversely to experiments performed on naked DNA, stress-specific p53 binding patterns were observed on chromatinized DNA using DLF. Altogether, these data indicate that chromatin affects p53′s interaction with REs and is important for the formation of p53 binding patterns.

UVB doses modulate p53 binding to the −2242 bp RE, and accessibility to this RE is affected by HATi Garcinol

We next decided to investigate how p53 binding patterns are modulated in cells following different UVB doses that induce distinct cellular outcomes. Using DLF, we compared p53 binding activities following 500 and 2000 J/m² UVB, which induce cell-cycle arrest and apoptosis, respectively. We observed that the −2242 bp RE was the only RE bound differently following these treatments (Figure 4A). As reported above, no specific modulation of p53 binding affinity was observed on naked DNA following 500 and 2000 J/m² UVB for this RE (Figure 2B). Since we observed that chromatin is important for the formation of p53 binding patterns, we investigated if chromatin remodeling, such as histone acetylation, could modulate p53′s interaction with REs. To this end, we used HATi Garcinol, which is a well-characterized inhibitor of histone acetyltransferases p300 and pCAF (22). wt fibroblasts were pre-treated for 2 h with 0–50 μM of Garcinol,
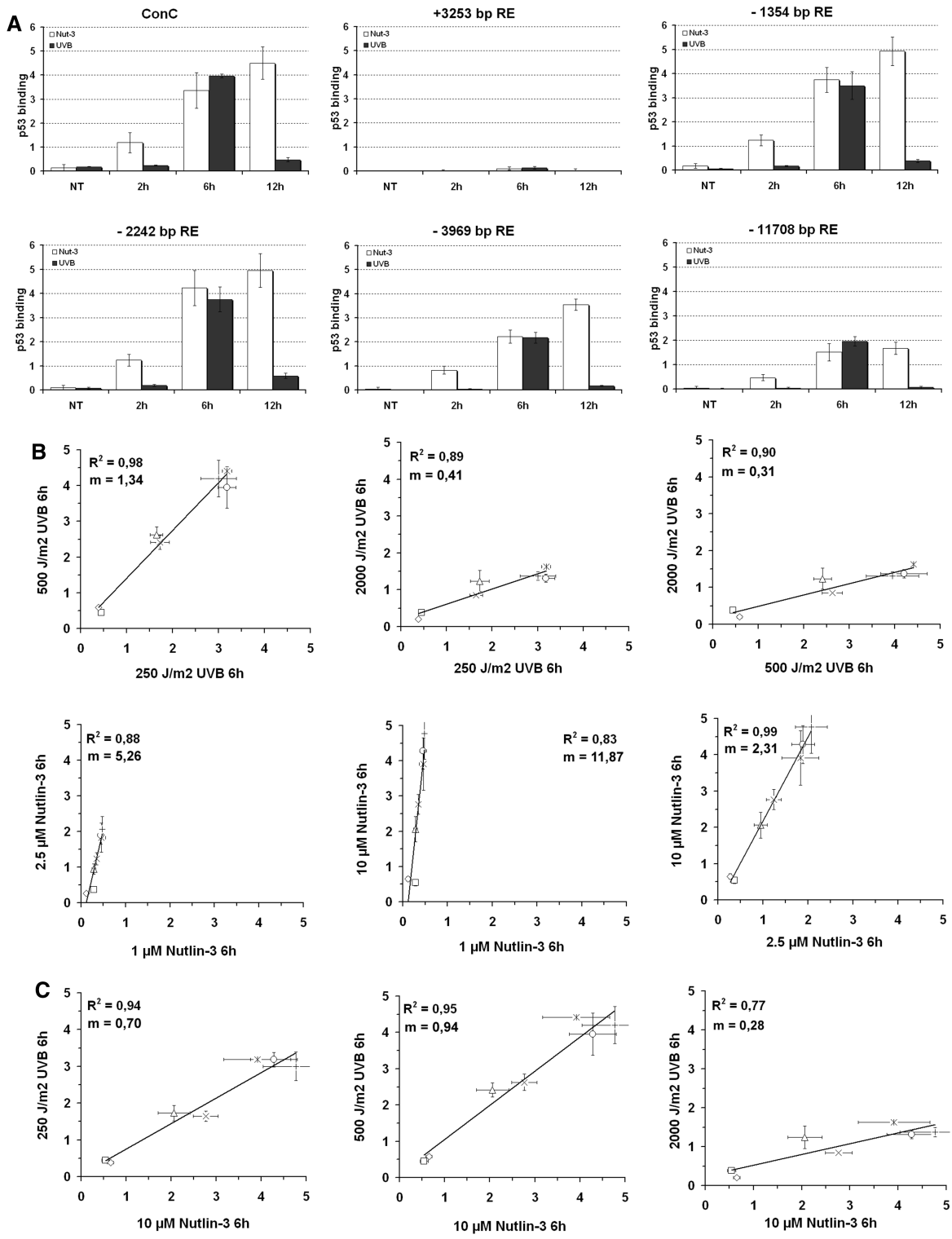
Figure 2. UVB and Nutlin-3 treatment doses lead to similar p53 binding patterns on naked DNA. (**A**) *In vitro* measurement of p53 binding activities using MAPD. wt fibroblasts were exposed to $500 \, J/m^2$ UVB or to $10 \, \mu M$ Nutlin-3 then collected at 2, 6 and 12 h for nuclear extract preparation. p53 binding to the REs located on *p21* and to the positive control sequence (ConC) was measured by MAPD. Binding measured on the negative control sequence (WRNC) was subtracted from values obtained for the other REs. Experiments were performed in triplicate and data are presented as mean ± SD. (**B**) Permutative comparisons of binding intensities measured by MAPD on the p53 REs located on *p21* following UVB and Nutlin-3 treatment. Each data set obtained at 6 h for a treatment dose was compared with the other doses using scatter plot representation. (**C**) Permutative comparisons between p53 binding intensities obtained following 250, 500 and $2000 \, J/m^2$ UVB and $10 \, \mu M$ Nutlin-3. Each data set obtained at 6 h for the three UVB doses was compared with the data set obtained at 6 h with $10 \, \mu M$ Nutlin-3. Nomenclature: open rectangle, WRNC; Ж, ConC; open rhombus, +3253 bp RE; open circle, −1354 bp RE; plus symbol, −2242 bp RE; Times symbol, −3969 bp RE; open triangle, −11 708 bp RE.

Figure 3. UVB and Nutlin-3 treatments induce stress-specific p53 binding patterns in cells on chromatin. wt and LF fibroblasts were exposed to UVB and Nutlin-3 then collected at 2, 6 and 12 h. p53 binding to the REs located on *p21* was then measured by ChIP (white) and DLF (black).
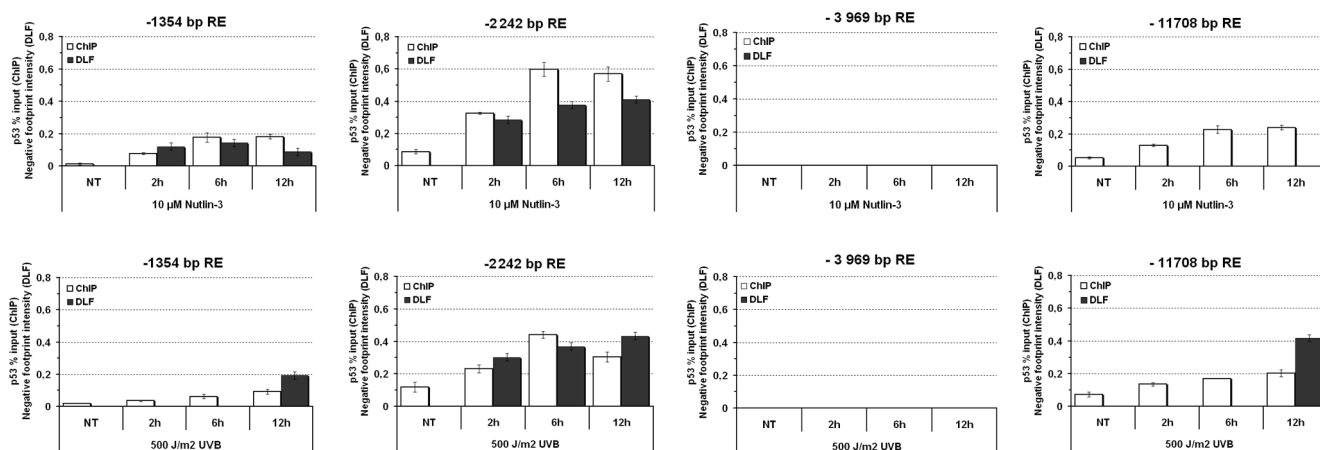
exposed to $500 \, J/m^2$ UVB, and then reincubated for 12 h in the presence of Garcinol before being collected. We first measured if Garcinol treatment affected p53 levels. We observed that this was not the case (Figure 4B). As p53 is a target of HAT and since acetylation of p53 might affect its interaction with REs, we used MAPD to determine whether HATi Garcinol had an effect on p53 binding activity on naked DNA. We observed that inhibition of HAT increased p53 binding activity to all REs on naked DNA as observed for the -2242 bp RE on Figure 4C. We then investigated the effect of HATi Garcinol on p53 binding activity on chromatinized DNA in cells. To this end, we monitored p53 binding to the -2242 bp RE in wt fibroblasts using DLF (Figure 4D and E). We observed that inhibition of HAT alone had no effect on the occupancy of the -2242 bp RE (Figure 4D compare lanes 5 and 6, Figure 4E). However, following UVB treatment, the occupancy of the -2242 bp RE strongly decreased as Garcinol concentration increased (Figure 4D and E); this was also confirmed by ChIP (Figure S7). Thus, in contrast to the results obtained on naked DNA, inhibition of HAT decreases p53 interaction with the -2242 bp RE in a chromatinized DNA context. To assess whether chromatin remodeling was affected by HATi Garcinol, we monitored histone H3 and H4 acetylation levels by ChIP (Figure 4F). At the actively bound -2242 bp RE, histones H3 and H4 were acetylated in non-stressed cells and acetylation increased following exposure to UVB. On the other hand, the acetylation level of histones located at the -3969 bp RE remained very low even after UVB irradiation. Interestingly, in the presence of HATi Garcinol a decrease in histone acetylation was observed. We thus concluded that p53′s interaction with REs is correlated with the acetylation level of histones.

DISCUSSION

How p53 achieves specific gene regulation in response to stress is an unresolved and exciting question in the field.

We and others recently showed that different stresses trigger different p53 binding patterns in primary cells (9,11). We demonstrated that p53 binds differently to the multiple REs located on the *p21* gene to regulate p21 variant transcriptions, revealing the crucial role of p53 binding patterns in the adaptive response to stress (11). However, the mechanism that produces these binding patterns remained largely unknown. Here, we showed that the formation of p53 binding patterns is not caused by a stress-dependent modulation of p53 binding affinity to RE sequences. Rather, we demonstrated that chromatin is needed for the formation of p53 binding patterns and that chromatin remodeling influences p53 interaction with REs.

Several lines of evidence support the view that posttranslational modifications of p53 and targeting co-factors direct p53 to bind to certain REs in a stress-dependent manner (12–19). The modulation of p53 binding affinity to specific RE sequences is one mechanism proposed to explain how posttranslational modifications and targeting co-factors direct p53 binding to generate p53 binding patterns. The results reported in this article suggest that this is not the case. The p53 binding patterns observed on naked DNA remained virtually identical following UVB and Nutlin-3 treatments, known to induce different p53 posttranslational modifications and leading to different cellular outcomes. This observation raises questions about how posttranslational modifications and targeting co-factors direct p53 binding. Since we only observed stress-specific p53 binding patterns within chromatin, we propose that posttranslational modifications and the targeting of co-factors most likely requires the presence of chromatin to influence p53 binding to certain REs. In support of this view, crosstalk between p53 modifications and histone H3 modifications have been recently observed, suggesting that histones might play a role in the regulation of p53 functions (36). Nevertheless, it has also been shown that p53 acetylated on Lys120 is specifically found at cell-cycle-arrest genes, but this modification is induced at a post-binding level
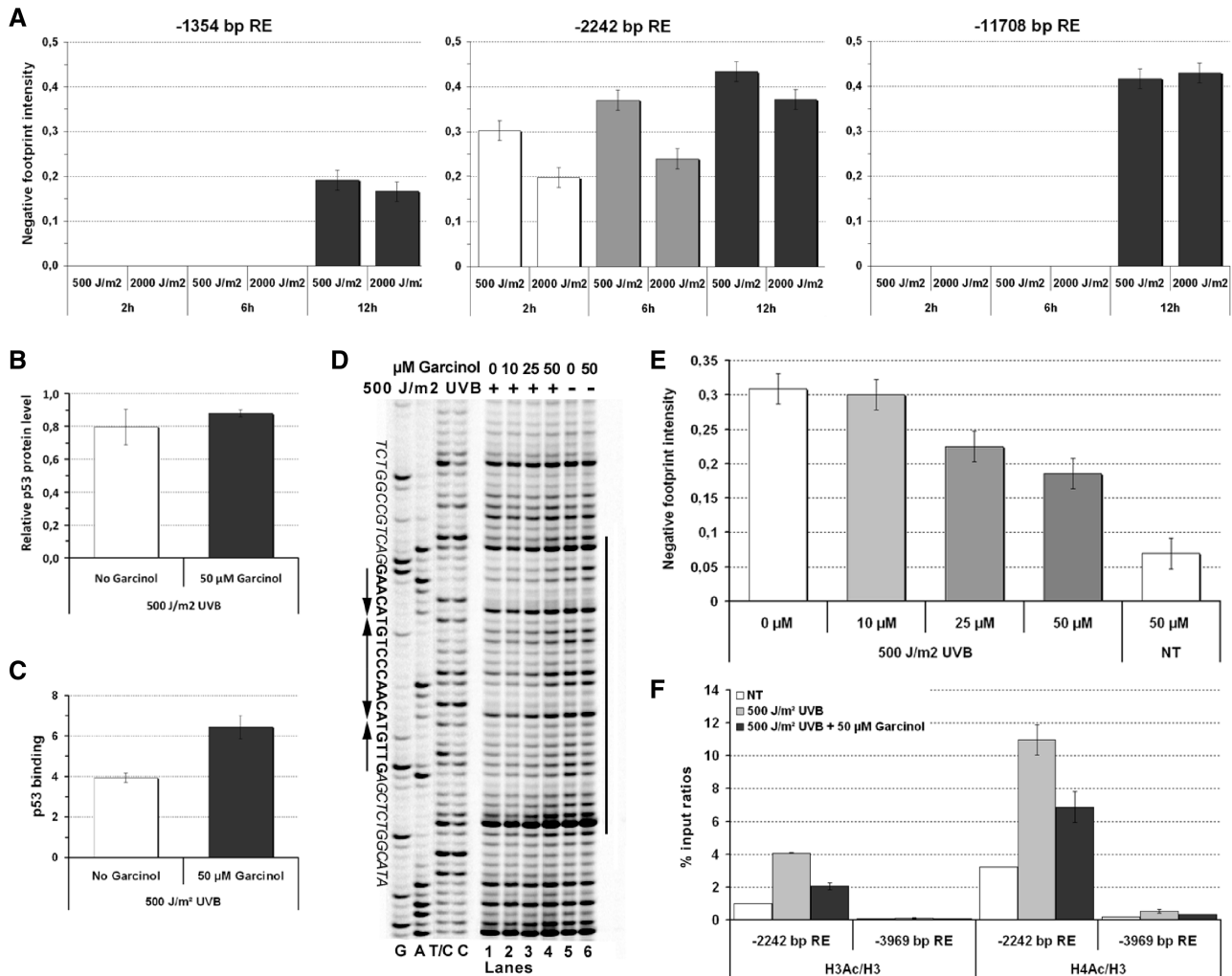
Figure 4. p53 binding to the –2242 bp RE is affected by HATi Garcinol. (**A**) Comparison of p53 binding activities on *p21* following UVB irradiation. p53 binding to the –1354, –2242 and –11 708 bp REs was measured by DLF in wt fibroblasts exposed to 500 and 2000 J/m² UVB. (**B**) Effect of Garcinol on p53 protein levels in wt fibroblasts exposed to UVB. p53 levels were measured by western blot. (**C**) Effect of Garcinol on p53 binding *in vitro* on naked DNA following UVB irradiation. p53 binding to the –2242 bp RE was measured by MAPD. (**D**) Effect of Garcinol on p53 binding in cells on chromatin following UVB irradiation. p53 binding to the –2242 bp RE was measured in wt fibroblasts using DLF. The gel obtained using an automated sequencer is presented, negative footprints are indicated by a bar. (**E**) Quantification of negative footprint intensity measured by DLF at the –2242 bp RE. (**F**) Effect of Garcinol on histone H3 and histone H4 acetylation following UVB irradiation. Levels of histone H3, acetylated histone H3 (H3Ac), and acetylated histone H4 (H4Ac) were measured by ChIP at the –2242 and –3969 bp REs. Results are expressed as ratios of acetylated histone on histone H3.

(37,38). Thus, an important point that needs to be addressed, regarding the role of posttranslational modifications in p53 targeting, is whether they effectively direct p53 to specific REs or whether they are induced at specific REs as a post-binding event.

One admitted view is that binding affinity and protein concentration are two crucial factors regulating protein interactions with DNA. Indeed, if binding affinity is high, the protein will bind even if it is present at a lower concentration. While on the other hand, if the binding affinity is low, the protein will bind if the concentration is high (6). Since we did not observe a stress-dependent modulation of p53 binding affinity to specific RE, this suggests that regulation of concentration might be a more important factor than regulation of affinity for controlling p53 binding. Interestingly, we observed a

global regulation of p53 binding activity to REs on naked DNA. Indeed, p53 binding to all REs was virtually abrogated 12 h following UVB exposure, even if p53 levels remained high. Interestingly, a regulatory mechanism of this kind might be useful to stop the p53 response to stress. Nevertheless, while we observed a global decrease in p53 binding activity, we found that high levels of p53 bound to REs were maintained in cells. Thus, despite the loss of binding activity of late accumulated p53, REs remained occupied by p53 induced at early response stages. This indicates that the global inhibition of p53 binding only circumvents p53 interaction with new REs, which might be a mechanism to prevent the regulation of novel p53 effector genes.

Of note, our results revealed that chromatin is needed for the modulation of p53's binding to REs and the

Figure 5. Models for selective p53 binding. In the model presented in (**A**), the formation of p53 binding patterns is driven by the binding affinity of p53 for RE sequences. It is proposed that p53 binding affinity to REs is modulated by stress-specific posttranslational modifications that favor binding to certain REs (red). In this model, p53 binding patterns should be observed on naked DNA. However, in our experimental setting, p53 binding patterns were virtually identical on naked DNA following the different treatments tested. We thus propose another model (**B**) where the affinity of p53 for specific RE sequences is not modulated differently following stresses, rather, the selectivity of p53 binding is dependent on the remodeling of chromatin (e.g. histone acetylation) at certain REs (red).

formation of p53 binding patterns. This is particularly well illustrated by the absence of p53 binding to the −11 708 bp RE following Nutlin-3 or to the −3969 bp RE following UVB and Nutlin-3 treatments in cells. Regarding the −3969 bp RE, the absence of binding in cells clearly indicates that accessibility to this RE seems to be blocked in a chromatinized context. It is noteworthy that stress-specific p53 binding to the −11 708 bp RE was only revealed by DLF and not by ChIP. We ruled out any sensitivity issue of DLF and attributed this discrepancy to the ability of p53 to interact with other DNA-binding proteins such as SP1 and WT1 (39,40). Interestingly, a potential SP1 RE (5′-ggGGGCTGTGTaggt-3) is located close to the −11 708 bp RE at −12 007 bp. Thus, if p53 locates only at the SP1 RE, ChIP might not be able to differentiate between binding to the −11 708 bp p53 RE and binding to the −12 007 bp SP1 RE, since DNA fragments encompassing both sites could have been immunoprecipitated. This might explain the conflicting ChIP and DLF data and shows the limitations of each technique and the advantage of combining both approaches.

One intriguing question is the role of the multiple REs present in the *p21* promoter. We and others proposed that the −1354 and −2242 bp REs might be involved in the regulation of p21 variant transcription (11,41). The proximity of the −11 709 bp RE to the *p21* gene also suggests that it might act as a distal regulator through DNA looping (11). However, Huarte *et al.* (42) recently showed that this RE is involved in the regulation of an intergenic non-coding RNA that favors apoptosis. Interestingly, both functions for the −11 708 bp RE might not be mutually exclusive and we think that a co-dependent regulation of both loci could provide a

mechanism to select between cell-cycle arrest and apoptosis outcomes.

Finally, the involvement of chromatin remodeling in the modulation of p53 binding to REs was strongly reinforced by the observation that the inhibition of histone acetylation by HATi Garcinol correlates with a decrease of p53 binding to REs in response to stress. Since histone modifications and chromatin remodeling do occur in a stress-specific manner (43), we propose that the formation of stress-specific p53 binding patterns could be directed by the remodeling of chromatin (e.g. histone acetylation). For example, the HAT p300 [which is recruited by p53 (44,45)], might only be active at certain promoters and thus increase histone acetylation levels to maintain p53 interaction only at specific REs. We thus propose a model in which chromatin acts as a filter to allow p53 binding to specific REs, over a model in which p53 binding patterns are caused by the modulation of p53's affinity to specific REs (Figure 5). Interestingly, the deregulation of histone modification and chromatin remodeling does occur during the carcinogenesis process (46,47). In the perspective provided by our results, this indicates that cancerous cells are capable of disrupting p53 binding patterns and in consequence p53's response to stress. This mechanism may disrupt the p53 pathway in p53$^{+/+}$ cancerous cells and explain why p53 binding patterns differ between cancer cells and primary cells (9–11).

SUPPLEMENTARY DATA

Supplementary Data are available at NAR Online.

REFERENCES

1. Millau,J.F., Bastien,N. and Drouin,R. (2009) P53 transcriptional activities: a general overview and some thoughts. *Mutat. Res.*, **681**, 118–133.
2. el-Deiry,W.S., Kern,S.E., Pietenpol,J.A., Kinzler,K.W. and Vogelstein,B. (1992) Definition of a consensus binding site for p53. *Nat. Genet.*, **1**, 45–49.
3. Riley,T., Sontag,E., Chen,P. and Levine,A. (2008) Transcriptional control of human p53-regulated genes. *Nat. Rev. Mol. Cell. Biol.*, **9**, 402–412.
4. Vousden,K.H. and Lu,X. (2002) Live or let die: the cell's response to p53. *Nat. Rev. Cancer*, **2**, 594–604.
5. Vousden,K.H. and Prives,C. (2009) Blinded by the light: the growing complexity of p53. *Cell*, **137**, 413–431.
6. Pan,Y., Tsai,C.J., Ma,B. and Nussinov,R. (2010) Mechanisms of transcription factor selectivity. *Trends Genet.*, **26**, 75–83.
7. Wei,C.L., Wu,Q., Vega,V.B., Chiu,K.P., Ng,P., Zhang,T., Shahab,A., Yong,H.C., Fu,Y., Weng,Z. *et al.* (2006) A global map of p53 transcription-factor binding sites in the human genome. *Cell*, **124**, 207–219.
8. Espinosa,J.M. (2008) Mechanisms of regulatory diversity within the p53 transcriptional network. *Oncogene*, **27**, 4013–4023.
9. Shaked,H., Shiff,I., Kott-Gutkowski,M., Siegfried,Z., Haupt,Y. and Simon,I. (2008) Chromatin immunoprecipitation-on-chip reveals stress-dependent p53 occupancy in primary normal cells but not in established cell lines. *Cancer Res.*, **68**, 9671–9677.
10. Millau,J.F., Mai,S., Bastien,N. and Drouin,R. (2010) p53 functions and cell lines: have we learned the lessons from the past? *BioEssays*, **32**, 392–400.
11. Millau,J.F., Bastien,N., Bouchard,E.F. and Drouin,R. (2009) p53 Pre- and post-binding event theories revisited: stresses reveal specific and dynamic p53-binding patterns on the p21 gene promoter. *Cancer Res.*, **69**, 8463–8471.
12. Oda,K., Arakawa,H., Tanaka,T., Matsuda,K., Tanikawa,C., Mori,T., Nishimori,H., Tamai,K., Tokino,T., Nakamura,Y. *et al.* (2000) p53AIP1, a potential mediator of p53-dependent apoptosis, and its regulation by Ser-46-phosphorylated p53. *Cell*, **102**, 849–862.
13. Knights,C.D., Catania,J., Di Giovanni,S., Muratoglu,S., Perez,R., Swartzbeck,A., Quong,A.A., Zhang,X., Beerman,T., Pestell,R.G. *et al.* (2006) Distinct p53 acetylation cassettes differentially influence gene-expression patterns and cell fate. *J. Cell. Biol.*, **173**, 533–544.
14. Samuels-Lev,Y., O'Connor,D.J., Bergamaschi,D., Trigiante,G., Hsieh,J.K., Zhong,S., Campargue,I., Naumovski,L., Crook,T. and Lu,X. (2001) ASPP proteins specifically stimulate the apoptotic function of p53. *Mol. Cell*, **8**, 781–794.
15. Bergamaschi,D., Samuels,Y., O'Neil,N.J., Trigiante,G., Crook,T., Hsieh,J.K., O'Connor,D.J., Zhong,S., Campargue,I., Tomlinson,M.L. *et al.* (2003) iASPP oncoprotein is a key inhibitor of p53 conserved from worm to human. *Nat. Genet.*, **33**, 162–167.
16. Bergamaschi,D., Samuels,Y., Sullivan,A., Zvelebil,M., Breyssens,H., Bisso,A., Del Sal,G., Syed,N., Smith,P., Gasco,M. *et al.* (2006) iASPP preferentially binds p53 proline-rich region and modulates apoptotic function of codon 72-polymorphic p53. *Nat. Genet.*, **38**, 1133–1141.
17. Budhram-Mahadeo,V.S., Bowen,S., Lee,S., Perez-Sanchez,C., Ensor,E., Morris,P.J. and Latchman,D.S. (2006) Brn-3b enhances the pro-apoptotic effects of p53 but not its induction of cell cycle arrest by cooperating in trans-activation of bax expression. *Nucleic Acids Res.*, **34**, 6640–6652.
18. Budram-Mahadeo,V., Morris,P.J. and Latchman,D.S. (2002) The Brn-3a transcription factor inhibits the pro-apoptotic effect of p53 and enhances cell cycle arrest by differentially regulating the activity of the p53 target genes encoding Bax and p21(CIP1/Waf1). *Oncogene*, **21**, 6123–6131.
19. Das,S., Raj,L., Zhao,B., Kimura,Y., Bernstein,A., Aaronson,S.A. and Lee,S.W. (2007) Hzf Determines cell survival upon genotoxic stress by modulating p53 transactivation. *Cell*, **130**, 624–637.
20. Noureddine,M.A., Menendez,D., Campbell,M.R., Bandele,O.J., Horvath,M.M., Wang,X., Pittman,G.S., Chorley,B.N., Resnick,M.A. and Bell,D.A. (2009) Probing the functional impact of sequence variation on p53-DNA interactions using a novel microsphere assay for protein-DNA binding with human cell extracts. *PLoS Genet.*, **5**, e1000462.
21. Li,B., Carey,M. and Workman,J.L. (2007) The role of chromatin during transcription. *Cell*, **128**, 707–719.
22. Balasubramanyam,K., Altaf,M., Varier,R.A., Swaminathan,V., Ravindran,A., Sadhale,P.P. and Kundu,T.K. (2004) Polyisoprenylated benzophenone, garcinol, a natural histone acetyltransferase inhibitor, represses chromatin transcription and alters global gene expression. *J. Biol. Chem.*, **279**, 33716–33726.
23. Rochette,P.J., Bastien,N., Lavoie,J., Guerin,S.L. and Drouin,R. (2005) SW480, a p53 double-mutant cell line retains proficiency for some p53 functions. *J. Mol. Biol.*, **352**, 44–57.
24. Jordan,J.J., Menendez,D., Inga,A., Noureddine,M., Bell,D.A. and Resnick,M.A. (2008) Noncanonical DNA motifs as transactivation targets by wild type and mutant p53. *PLoS Genet.*, **4**, e1000104.
25. Cho,Y., Gorina,S., Jeffrey,P.D. and Pavletich,N.P. (1994) Crystal structure of a p53 tumor suppressor–DNA complex: understanding tumorigenic mutations. *Science*, **265**, 346–355.
26. Inga,A., Storici,F., Darden,T.A. and Resnick,M.A. (2002) Differential transactivation by the p53 transcription factor is highly dependent on p53 level and promoter target sequence. *Mol. Cell. Biol.*, **22**, 8612–8625.
27. Gevry,N., Chan,H.M., Laflamme,L., Livingston,D.M. and Gaudreau,L. (2007) p21 transcription is regulated by differential localization of histone H2A.Z. *Genes Dev.*, **21**, 1869–1881.
28. Drouin,R., Therrien,J.P., Angers,M. and Ouellet,S. (2001) In vivo DNA analysis. *Methods Mol. Biol.*, **148**, 175–219.
29. Olsson,A., Manzl,C., Strasser,A. and Villunger,A. (2007) How important are post-translational modifications in p53 for selectivity in target-gene transcription and tumour suppression? *Cell Death Differ.*, **14**, 1561–1575.
30. Vassilev,L.T., Vu,B.T., Graves,B., Carvajal,D., Podlaski,F., Filipovic,Z., Kong,N., Kammlott,U., Lukacs,C., Klein,C. *et al.* (2004) In vivo activation of the p53 pathway by small-molecule antagonists of MDM2. *Science*, **303**, 844–848.
31. Thompson,T., Tovar,C., Yang,H., Carvajal,D., Vu,B.T., Xu,Q., Wahl,G.M., Heimbrook,D.C. and Vassilev,L.T. (2004) Phosphorylation of p53 on key serines is dispensable for

transcriptional activation and apoptosis. *J. Biol. Chem.*, **279**, 53015–53022.

32. el-Deiry,W.S., Tokino,T., Waldman,T., Oliner,J.D., Velculescu,V.E., Burrell,M., Hill,D.E., Healy,E., Rees,J.L., Hamilton,S.R. *et al.* (1995) Topological control of p21WAF1/CIP1 expression in normal and neoplastic tissues. *Cancer Res.*, **55**, 2910–2919.

33. Saramaki,A., Banwell,C.M., Campbell,M.J. and Carlberg,C. (2006) Regulation of the human p21(waf1/cip1) gene promoter via multiple binding sites for p53 and the vitamin D3 receptor. *Nucleic Acids Res.*, **34**, 543–554.

34. Nozell,S. and Chen,X. (2002) p21B, a variant of p21(Waf1/Cip1), is induced by the p53 family. *Oncogene*, **21**, 1285–1294.

35. Drouin,R., Bastien,N., Millau,J.F., Vigneault,F. and Paradis,I. (2009) In cellulo DNA analysis (LMPCR footprinting). *Methods Mol. Biol.*, **543**, 293–336.

36. Warnock,L.J., Adamson,R., Lynch,C.J. and Milner,J. (2008) Crosstalk between site-specific modifications on p53 and histone H3. *Oncogene*, **27**, 1639–1644.

37. Sykes,S.M., Mellert,H.S., Holbert,M.A., Li,K., Marmorstein,R., Lane,W.S. and McMahon,S.B. (2006) Acetylation of the p53 DNA-binding domain regulates apoptosis induction. *Mol. Cell*, **24**, 841–851.

38. Tang,Y., Luo,J., Zhang,W. and Gu,W. (2006) Tip60-dependent acetylation of p53 modulates the decision between cell-cycle arrest and apoptosis. *Mol. Cell*, **24**, 827–839.

39. Koutsodontis,G., Tentes,I., Papakosta,P., Moustakas,A. and Kardassis,D. (2001) Sp1 plays a critical role in the transcriptional activation of the human cyclin-dependent kinase inhibitor p21(WAF1/Cip1) gene by the p53 tumor suppressor protein. *J. Biol. Chem.*, **276**, 29116–29125.

40. Zhan,Q., Chen,I.T., Antinore,M.J. and Fornace,A.J. Jr (1998) Tumor suppressor p53 can participate in transcriptional induction of the GADD45 promoter in the absence of direct DNA binding. *Mol. Cell. Biol.*, **18**, 2768–2778.

41. Radhakrishnan,S.K., Gierut,J. and Gartel,A.L. (2006) Multiple alternate p21 transcripts are regulated by p53 in human cells. *Oncogene*, **25**, 1812–1815.

42. Huarte,M., Guttman,M., Feldser,D., Garber,M., Koziol,M.J., Kenzelmann-Broz,D., Khalil,A.M., Zuk,O., Amit,I., Rabani,M. *et al.* A large intergenic noncoding RNA induced by p53 mediates global gene repression in the p53 response. *Cell*, **142**, 409–419.

43. Johnson,A.B. and Barton,M.C. (2007) Hypoxia-induced and stress-specific changes in chromatin structure and function. *Mutat. Res.*, **618**, 149–162.

44. Avantaggiati,M.L., Ogryzko,V., Gardner,K., Giordano,A., Levine,A.S. and Kelly,K. (1997) Recruitment of p300/CBP in p53-dependent signal pathways. *Cell*, **89**, 1175–1184.

45. Espinosa,J.M. and Emerson,B.M. (2001) Transcriptional regulation by p53 through intrinsic DNA/chromatin binding and site-directed cofactor recruitment. *Mol. Cell*, **8**, 57–69.

46. Fog,C.K., Jensen,K.T. and Lund,A.H. (2007) Chromatin-modifying proteins in cancer. *Apmis*, **115**, 1060–1089.

47. Thorne,J.L., Campbell,M.J. and Turner,B.M. (2009) Transcription factors, chromatin and cancer. *Int. J. Biochem. Cell. Biol.*, **41**, 164–175.